Materials Advances

ROYAL SOCIETY OF CHEMISTRY

PAPER

View Article Online
View Journal | View Issue

Cite this: *Mater. Adv.*, 2026, 7, 2241

Using sulfuric acid–phosphoric acid leaching to remove aluminum and cathode material metal residues from spent graphite

Venla Rantala, †[a] Toni Kauppinen,†[ab] Tao Hu, [a] Ali Huerta Flores,[a] Anne Heponiemi, [a] Ulla Lassi [ab] and Sari Tuomikoski *[a]

Spent graphite (SG) separated in industrial-scale recycling of spent lithium-ion batteries (LIBs) usually contains various impurities, such as cathode material metals, aluminum, and organic contaminants. Therefore, the re-use of SG may require various purification and regeneration processes to meet battery-grade purity requirements. This study investigated the simultaneous removal of aluminum and cathode material metals (lithium, nickel, manganese, and cobalt) from LIB black mass-derived SG using a sulfuric acid–phosphoric acid mixture for leaching. The effects of phosphoric acid concentration (0–0.7 mol L^{-1}) and reaction time (240–600 min) were evaluated. Cathode material metals were removed with sulfuric acid leaching (97.5–98.9%), but aluminum impurities remained almost completely in the SG (aluminum removal: 17.8%). The simultaneous removal of the studied elements was achieved by a sulfuric acid–phosphoric acid mixture. The removal of studied elements was significantly enhanced by increasing phosphoric acid concentration from 0.1 mol L^{-1} to 0.5 mol L^{-1} and by increasing reaction time from 240 min to 600 min. Under the studied conditions (sulfuric acid: 2.75 mol L^{-1}; phosphoric acid: 0.5 mol L^{-1}; time: 600 min; temperature: 100 °C; L/S ratio: 10 mL g^{-1}), aluminum removal was increased to 90.8%, while cathode material metals were removed between 97.7% and 99.5%. The carbon content of the SG sample notably increased from 69.2 to 93.0 wt% with this single-stage acid mixture leaching process. Based on thermogravimetric and X-ray photoelectron spectroscopy analyses, residual impurities in the purified SG sample consisted mostly of organic or other volatile impurities. In addition, lithium phosphate, produced as a side stream in lithium processing, was also examined as an alternative phosphate source in the acid mixture to replace phosphoric acid. Based on the results, the sulfuric acid–lithium phosphate mixture showed equal capability for aluminum and cathode material metal removal to the sulfuric acid–phosphoric acid mixture, increasing carbon content up to 92.3 wt%. This offers a potential application for further lithium phosphate use. The results of this study showed that a sulfuric acid–phosphoric acid mixture has a good capability to purify SG, and side stream-based lithium phosphate can replace phosphoric acid in the mixture.

Received 22nd October 2025,
Accepted 5th January 2026

DOI: 10.1039/d5ma01222h

rsc.li/materials-advances

1. Introduction

Battery waste from electric vehicles and portable electronics increases yearly due to the increased consumption of lithium-ion batteries (LIBs). In Europe, the amount of spent batteries exceeds more than 1.9 million tonnes annually.[1] Spent LIBs contain various valuable materials that are critical to recovery *via* recycling processes. Industrial-scale recycling processes of spent LIBs include pretreatment processes (discharge, dismantling, separation, *etc.*), after which hydrometallurgical and pyrometallurgical processes take place.[2] LIBs can also be recycled *via* direct recycling methods, but they have yet to be commercialized due to their financial infeasibility.[3] However, the collection rates for LIBs are low in the European Union (EU), and among the other 35 kilotonnes of portable batteries containing hazardous substances end up in municipal waste.[1] This leads to the loss of valuable resources that are needed for increasing demand.

Current recycling processes focus on the recovery of valuable metals (cobalt, nickel, and copper). The anode active material (graphite) is not recovered, and almost no lithium is recovered.[1] In LIBs, graphite may originate from natural resources or be

[a] *University of Oulu, Research Unit of Sustainable Chemistry, P.O. Box 4300, Oulu, FI-90014, Finland. E-mail: sari.tuomikoski@oulu.fi*
[b] *University of Jyvaskyla, Kokkola University Consortium Chydenius, Talonpojankatu 2 B, FI-67100 Kokkola, Finland*
† Dual-first authorship,.

artificially produced.[4] The production of artificial graphite requires substantial amounts of energy, while natural graphite has been classified as a strategically critical material.[5] LIB cells typically contain 12–21 wt% graphite; therefore, the increasing consumption of LIBs generates a significant amount of spent graphite (SG).[6] The overall life cycle of batteries should have a low carbon footprint to maximize the potential to reduce carbon emissions in the mobility and energy storage sectors. Therefore, the European Parliament and the Council have provided regulation (EU) 2023/1542 (2023, July 12) on carbon footprint declaration.[7] Recovering and reusing SG is important from both environmental and economic perspectives.

At the laboratory scale, an anode electrode is often manually separated from discharged LIBs.[8–16] The manually separated anode electrode contains impurities such as copper from the current collector, binder, and electrolyte. In industrial-scale processes, the mechanical crushing of spent LIBs produces a black mass containing anode- and cathode-active materials. Separating an anode from a cathode may be done, for example, by flotation[6] or leaching.[17,18] The challenge with black mass-derived SG is that it usually contains various impurities, such as residues from cathode material metals (lithium, nickel, manganese, cobalt, *etc.*), current collectors (aluminum and copper), and organic contaminants (binder, organic solvents, *etc.*), requiring further purification. For recovered graphite to be reused in batteries, impurities must be removed as much as possible, as they affect electrochemical performance.[19]

Purification and regeneration of separated SG are often divided into hydrometallurgical,[8–11,20] pyrometallurgical,[12–14] and combination[15,16,21–24] treatments. Most studies focus on the purification of the manually separated SG.[8–16] Manually separated graphite contains fewer impurities compared to black mass-derived SG. However, manual separation of SG electrodes is not feasible in industrial-sized processes. The literature does not provide comprehensive information on removing impurities from industrial black mass-derived SG. Only a few publications exist on the purification and regeneration of such SG.[20,21,23,25] Chang *et al.*[20] used sulfuric acid and hydrogen peroxide to separate graphite and lithium manganate, upgrading the carbon content of SG from 34.2 to 97.62 wt%. Gao *et al.*[21] used a sulfation roasting–acid leaching process to remove lithium iron phosphate residues from SG, increasing carbon content from 88.07 to 98.91 wt%.

One of the main impurities in industrial SG samples are cathode active material residues,[20,21,23,25] which are easy to remove using a simple sulfuric acid leaching treatment with hydrogen peroxide.[25] However, aluminum, particularly aluminum oxide hydroxide (boehmite) phase, has turned out to be a challenge in the sulfuric acid leaching treatment.[18,25] In our previous study,[25] different purification processes (hydrometallurgical leaching treatments, thermal treatments, and combination treatments) were compared for two SG obtained from industrial-scale processes. The SG samples contained various impurities, mainly residues from cathode active material and aluminum. The results showed that cathode material metals were easily removed (97.2–98.9%) by sulfuric acid leaching with and without the addition of hydrogen peroxide; however, only a maximum of 11.2% aluminum was removed. Aluminum removal required additional sodium hydroxide leaching or thermal treatment. Another option is to convert aluminum impurities in SG into water-soluble complex ions using ammonium fluoride.[26] Hydrochloric acid with sodium fluoride has also been utilized for the removal of aluminum and other impurities from natural graphite. In the latter process, sodium fluoride generates hydrofluoric acid, which removes most silicate impurities.[27] More commonly, oxides containing metals with high oxidation states and elemental metals have been converted into water-soluble sulfates by the sulfation roasting process.[21,24,28] To make SG purification industrially reasonable, the number of process steps should be kept to a minimum. Environmental considerations should be considered, such as avoiding the use of halogen-containing chemicals.

Phosphoric acid is a suitable leaching agent for aluminum. Zhang *et al.*[29] used a sulfuric acid–phosphoric acid mixture to extract aluminum and lithium from bauxite mine tailings. Shukla *et al.*[30] applied phosphoric acid to recycle aluminum from pharmaceutical blister packages. In these studies, high aluminum leaching efficiencies (88.6–100%) were achieved. Furthermore, phosphoric acid has been utilized as a leaching and precipitating agent to recover valuable metals (lithium, nickel, manganese, and cobalt) from spent LIB materials.[31–34] Phosphoric acid could also be utilized to remove aluminum residues from SG. However, other impurities in SG may form insoluble precipitates with phosphoric acid, but this can be avoided by adjusting the pH value using other acids.[33] Sulfuric acid is generally used as a leaching agent for cathode material metals.[35–37] To our knowledge, there are no studies available where a sulfuric acid–phosphoric acid mixture has been utilized to purify SG from aluminum and cathode material metal residues. The use of a sulfuric acid–phosphoric acid mixture could allow metals to be removed simultaneously from SG, minimizing the needed process steps.

In addition to phosphoric acid, lithium phosphate could be a potential source of phosphate in the mixture. Lithium carbonate precipitation usually leaves noticeable lithium concentrations after lithium carbonate recovery. Lithium phosphate has a significantly lower solubility in water solutions than lithium carbonate, and phosphate is often used to recover lithium from low-concentration solutions.[38] There are not many applications of precipitated lithium phosphate, and the market demand is small.[39] Several conversion reactions have been proposed to convert lithium from lithium phosphate into soluble lithium compounds and solid phosphate products. Shin *et al.*[40] proposed leaching lithium using a calcium chloride solution to produce an aqueous lithium chloride solution and a solid calcium phosphate precipitate. Additionally, the presence of iron(III) ions in the acidic lithium phosphate solution separates phosphate from the solution forming solid iron phosphate and leaving lithium in the solution.

The objective of this study was to examine whether it is possible to increase the simultaneous removal of aluminum and cathode material metals (lithium, nickel, manganese, and

cobalt) from LIB black mass-derived SG. This study first time proved that a sulfuric acid–phosphoric acid mixture can be used for the SG purification process. This single-stage purification process minimizes needed purification steps without the use of halogen-containing chemicals, offering a simple, industrially reasonable option for SG purification. This study also proved the possible application of lithium phosphate as an alternative phosphate source in the mixture, considering circular economy insight. Lithium phosphate is a common side stream of lithium processes but lacks proper application targets. Use as a phosphate source in the SG purification process could offer a potential application for further use.

2. Experimental section

2.1. Materials and reagents

A Nordic recycling company provided SG from spent LIB black mass. In our previous study,[25] the untreated SG was analyzed and characterized. Table 1 shows the impurity contents of selected elements and the carbon content of the untreated SG sample measured by inductively coupled plasma–optical emission spectrometry (ICP–OES) and an elemental CHNS(O) analyzer.

In the leaching, laboratory reagent grade sulfuric acid (≥95%; Fisher Scientific) and analytical grade *ortho*-phosphoric acid (85%; Merck KGaA) were used. Analytical reagent grade nitric acid (>69%; Honeywell), hydrochloric acid (37%; Fisher Chemical), hydrofluoric acid (40%; VWR Chemicals BDH), and boric acid (>99.8%; Fisher Scientific) were used to pretreat the solid samples (n = 2) using method 2 (published previously)[41] in a microwave before ICP–OES (Agilent 5110 VDV; Agilent Technologies, USA) analysis. Commercial battery-grade graphite (Hitachi Energy) was used as the reference sample. In the elemental CHNS(O) analysis, high-purity graphite (99.99 wt% carbon) (AR 2029, Alpha Resources) was used as a reference.

2.2. Preparation of lithium phosphate

Lithium phosphate was prepared from a lithium sulfate solution, which was a filtrate from cathode material precursor precipitation using lithium hydroxide as a precipitant. The lithium content of the solution was 10.6 g L^{-1}. A 1.5 mol L^{-1} phosphate solution was prepared by dissolving trisodium phosphate hydrate in 500 mL of 60 °C ion-exchanged water and adding dropwise to 500 mL of 50 °C lithium sulfate solution in a 1000 mL Duran baffled bottle. The mixture was agitated at 50 °C magnetically and allowed to react for 1 hour. The final pH of the reaction was 10.9. Solids were collected by vacuum filtration using Ahlsell-Munksjö 393 filter paper. The obtained lithium phosphate was washed and dried overnight at 105 °C. The phosphate content of the obtained powder was 24.5 wt%.

2.3. Experimental procedure

2.3.1. Purification *via* a sulfuric acid–phosphoric acid mixture. Sulfuric acid–phosphoric acid mixture was studied for SG purification. Based on a previous study[25] and preliminary experiments, high removals (>99%) for cathode material metals (lithium, nickel, manganese, cobalt) were obtained from the SG sample using a 2.75 mol L^{-1} sulfuric acid concentration. In addition, it adjusts the mixture's pH to <0, preventing the precipitation of insoluble phosphates. The sulfuric acid concentration was selected and kept constant, as the aim was to focus on the effect of phosphoric acid concentration on the simultaneous removal of aluminum and cathode material metals. The removal of metal impurities from SG was investigated at different reaction conditions described in Table 2. A mixture containing sulfuric acid (2.75 mol L^{-1}) and phosphoric acid (0–0.7 mol L^{-1}) was prepared in a volumetric flask. 50 mL of the prepared mixture was poured into a 250 mL three-neck round-bottom flask with a graduated flask. The round-bottom flask was equipped with a reflux condenser to prevent the evaporation of the solution. The mixture was heated and agitated (300 rpm) using a magnetic stirrer with a temperature control unit and a heating block (Hemispheric Bowl, Velp Scientifica). SG (5 g) was added to the flask when the temperature of the acid mixture reached 100 °C. The reaction temperature was chosen to be 100 °C, as high temperatures generally increase the reaction rate in the leaching processes,[42] and based on the previous study[25] where high removals of cathode material metals without hydrogen peroxide were obtained at 100 °C.

After the reaction (240–600 min), the solution was filtered (MN 640 w, Ø: 11 cm, retention 7–12 μm, Macherey-Nagel) by vacuum filtration. Ultrapure water (80 mL) was filtered through the SG to wash the remaining leachate. The volume of the solution containing both leachate and washing water was measured using a graduated flask. A sample from this solution was taken and filtered using a syringe filter (0.45 μm; fisherbrand PES). Elemental concentrations of aluminum, cobalt,

Table 1 Impurities of the untreated SG measured by ICP–OES after microwave-assisted acid digestion (replicates (n) = 3) and elemental CHNS(O) analyzer results (n = 3–4) (average (Av.) ± standard deviation (SD)). Source ref. 25

	ICP–OES (mg g^{-1} ± mg g^{-1})							Elemental analyzer (wt% ± wt%)				
	Al	Co	Cu	Li	Mn	Ni	P	N	C	H	S	O
Av.	27.90	35.57	1.68	5.80	33.70	36.03	0.619	0.1	69.2	0.5	1.5	9.4
SD	0.66	0.40	0.03	0.09	0.46	0.47	0.037	0.1	1.2	0.0	0.3	0.2

Table 2 Studied factors in the sulfuric acid–phosphoric acid leaching purification process of SG (temperature: 100 °C; L/S ratio: 10 mL g^{-1})

Studied factor	Sulfuric acid (mol L^{-1})	Phosphoric acid (mol L^{-1})	Reaction time (min)
Phosphoric acid (mol L^{-1})	2.75	0, 0.1, 0.3, 0.5, 0.7	240
Time (min)	2.75	0.5	240, 360, 480, 600

lithium, nickel, manganese, and phosphorus were measured from this solution using ICP–OES.

Removals R (%) of the studied elements were calculated using eqn (1):

$$R\,(\%) = \frac{c \cdot V}{C \cdot m} \times 100\%, \quad (1)$$

where c is the concentration (mg L^{-1}) of the studied element in the filtered solution, V is the final volume (L) of the solution, m is the weight (g) of the sample, and C is the initial concentration (mg g^{-1}) of the element in the SG sample (Table 1). Each experiment was replicated (n = 2).

2.3.2. Purification *via* a sulfuric acid–lithium phosphate mixture. Lithium phosphate was investigated as an alternative phosphate source to replace phosphoric acid in the acid mixture. The preparation of lithium phosphate is described in Section 2.2. Sulfuric acid (2.75 mol L^{-1})–lithium phosphate (0.1 mol L^{-1}, 0.3 mol L^{-1}, and 0.5 mol L^{-1}) mixtures were prepared in 50 mL volumetric flasks. The mass of lithium phosphate was calculated based on the phosphorus content measured by ICP–OES. Experiments were conducted as described in Section 2.3.1 using a reaction temperature of 100 °C, a reaction time of 240 or 600 min, and an L/S ratio of 10 mL g^{-1}. Each experiment was replicated (n = 2).

2.4. Analysis and characterization

Samples were analyzed using ICP–OES and an elemental CHNS(O) analyzer (FlashSmart™ Elemental Analyzer; Thermo Scientific, Italy). X-ray diffraction (XRD) patterns were collected at 40 mA and 45 kV, 2θ values from 6–90° with $CuK_{\alpha 1}$ radiation λ = 1.54060 Å and a step size of 0.0170° by PANalytical X'Pert Pro X-ray diffractometer (Malvern Panalytical, Almelo, Netherlands). The phases of the samples were identified using Highscore Plus software (Version 4.0, PANalytical B. V., Netherlands). The morphologies of the samples and elemental mapping were performed using field emission scanning electron microscopy (FESEM) with an energy dispersive X-ray spectrometer (EDS) (JEOL JSM-7900 F, JEOL Ltd, Tokyo, Japan). The FESEM was operated at 15 kV with a working distance of 10 mm. For the EDS mapping, AZtec software from Oxford Instruments was used. Thermogravimetric analysis (TGA) was performed with a NETZSCH STA 409PC/PG instrument under a nitrogen atmosphere at a 20 mL/min flow rate. The heating rate was 10 °C min^{-1} up to 1000 °C.

An attenuated total reflectance Fourier transform infrared (ATR-FTIR) spectrometer (Spectrum Two, PerkinElmer, United States) was employed with a germanium crystal to study the possible changes in functional groups. ATR-FTIR was performed with eight scans at 4000–400 cm^{-1} with a resolution of 4 cm^{-1}. The baseline was measured with potassium bromide (Merck). Samples were diluted with potassium bromide (1 : 100).

X-ray photoelectron spectroscopy (XPS) analysis was performed using a Thermo Fisher Scientific ESCALAB 250Xi XPS System at the Centre for Material Analysis, University of Oulu (Finland) to analyze surface species. The sample powders were placed on a gold sample holder. The high-resolution scan of an individual element used a pass energy of 20 eV, while the Survey scan used a pass energy of 150 eV. The monochromatic AlKα radiation (1486.7 eV) operated at 20 mA and 15 kV with an X-ray spot size of 650 μm. The measurement data were analyzed by the Avantage V5 program. Charge compensation was performed by applying the C1s peak at 284.8 eV as a reference. The peak fitting was performed with the standard method of Avantage (Smart background, TXFN) according to the "XPS Knowledge" coming together with the Avantage program.

3. Results and discussion

3.1. Effect of the sulfuric acid–phosphoric acid mixture on impurity removal

This study aims to investigate whether it is possible to simultaneously remove aluminum and cathode material metal (lithium, nickel, manganese, and cobalt) residues from SG using a sulfuric acid–phosphoric acid mixture to minimize the required purification steps. First, the effect of phosphoric acid concentration and reaction time is evaluated, after which the samples are characterized to understand the effect of the treatment. In Section 3.3, a common side stream, lithium phosphate, is investigated as an alternative phosphate source.

3.1.1. Effect of phosphoric acid concentration. Fig. 1 shows the effect of phosphoric acid concentration (0–0.7 mol L^{-1}) in the acid mixture on aluminum and cathode material metal removals from the SG. Other parameters were kept constant (Table 2). Without the addition of phosphoric acid, only 17.8% of the aluminum was removed. The results showed a significant increase in aluminum removal when the phosphoric acid concentration increased in the system. Even with a phosphoric acid concentration of 0.1 mol L^{-1} in the mixture, removal was 30.2%. The highest aluminum removal (67.2%) was obtained

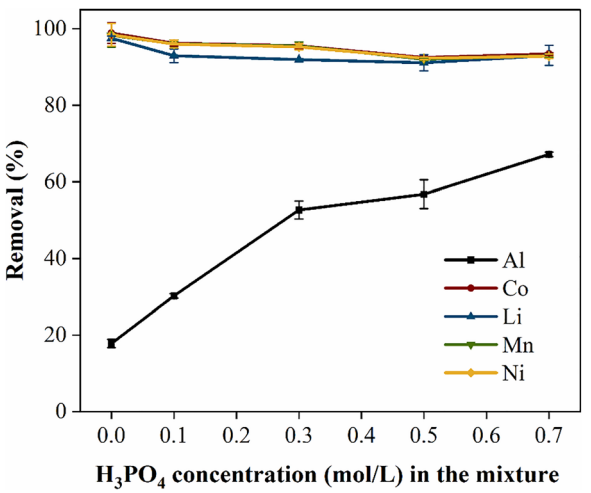

Fig. 1 Effect of phosphoric acid concentration (0–0.7 mol L^{-1}) on simultaneous impurity removal of aluminum and cathode material metals from SG by sulfuric acid–phosphoric acid mixture (other factors: sulfuric acid: 2.75 mol L^{-1}; time: 240 min; temperature: 100 °C; L/S ratio: 10 mL g^{-1}). Error bars represent experimental points of replicates (n = 2).

using a 0.7 mol L^{-1} concentration of phosphoric acid together with sulfuric acid (2.75 mol L^{-1}). This was expected as the reaction rate generally rises with increasing reactant concentrations.[42] An increase in phosphoric acid concentrations provides more phosphoric acid species that can complex aluminum. To minimize the phosphate content in the acid waste and avoid recyclability problems, a 0.5 mol L^{-1} phosphoric acid concentration was selected for the next step.

As mentioned in the introduction, the use of strong acid in the system is essential to adjust the pH for simultaneous cathode material removal from SG. At high pH values, cathode material metals may precipitate as insoluble phosphates. Based on the Yang *et al.*[33] study, even at pH 1.3, some metals can precipitate in the phosphoric acid system. Chen *et al.*[31] used phosphoric acid as a leaching and precipitating agent to separate lithium and cobalt from lithium cobalt oxide cathode material. The use of 0.7 mol L^{-1} phosphoric acid led to the precipitation of cobalt as cobalt phosphate, while lithium was left in the solution.[31] In SG purification studies, it is essential to remove all impurities from SG. Therefore, when phosphoric acid is used in the system to remove aluminum, the pH value must be adjusted to prevent the precipitation of insoluble compounds. Based on Fig. 1, the cathode material metals were removed almost completely in each experiment (see Table S1). The previous study[25] showed that 0.5 and 5 mol L^{-1} sulfuric acid concentrations may also be sufficient for cathode material metal removals, depending on the other leaching conditions. This study aimed to focus on the effect of phosphoric acid, and therefore, the sulfuric acid was kept constant at a high concentration sufficient to remove cathode material metals and prevent the precipitation of insoluble phosphates.

The phosphoric acid's ability to dissolve aluminum may be due to the complex formation.[29,30,43] In the sulfuric acid–phosphoric acid mixture, sulfuric acid provides a strongly acidic environment. Dissociation eqn (2) and (3), and (4) show the dissociation of phosphoric acid and corresponding dissociation constant values as negative logarithm (pK_a) at 25 °C.[44]

$$H_3PO_4 \rightleftharpoons H^+ + H_2PO_4^-, \quad pK_{a_1} = 2.16 \qquad (2)$$

$$H_2PO_4^- \rightleftharpoons H^+ + HPO_4^{2-}, \quad pK_{a_2} = 7.21 \qquad (3)$$

$$HPO_4^{2-} \rightleftharpoons H^+ + PO_4^{3-}, \quad pK_{a_3} = 12.31 \qquad (4)$$

In the sulfuric acid–phosphoric acid system, 2.75 mol L^{-1} sulfuric acid provides strongly acidic conditions. Based on the pK_{a_1} value, phosphoric acid exists mostly in phosphoric acid form (pH value <0). According to Zhou *et al.*[32] the percent content of phosphoric acid is 0.993, and in that the content of dihydrogen phosphate is 0.007 at pH 0. Zhang *et al.*[29] used a sulfuric acid–phosphoric acid mixture to leach aluminum and lithium from bauxite mine tailings. Based on the study, phosphoric acid and dihydrogen phosphate can coordinate metals, producing complexes.[29] Similarly, Shukla *et al.*[30] suggested that the aluminum phosphate complex (*i.e.*, $Al(H_2PO_4)_3$) is formed when aluminum is leached from waste blister packages using phosphoric acid. These studies are supported by the Mortlock *et al.*[43] study, where aluminum–phosphoric acid complexes under acidic conditions (pH $\leq$ 1.5) were determined. Based on the study, several possible complexes may exist. Aluminum can be complexed, *i.e.*, to H_3PO_4, $H_2PO_4^-$, $H_6P_2O_8$, and $H_5P_2O_7^-$ ligands. The pH value of the solution and the concentrations affect which complexes are dominant.[43] It is suggested that the removal of aluminum from SG by sulfuric acid–phosphoric acid mixture is similarly due to complex formation in acidic conditions with phosphoric acid species.

3.1.2 Effect of reaction time. The effect of reaction time (240–600 min) was investigated to avoid the need for a higher phosphoric acid concentration in the system. Fig. 2 shows the effect of reaction time (240–600 min) on aluminum and cathode material metal removals from the SG. Other parameters were kept constant (Table 2). The results show that by increasing the reaction time from 240 min to 600 min, the aluminum was almost completely removed. The removal increased from 56.8% to 90.8%. Also, the cathode material metals were removed almost completely (97.7–99.5%) (Table S2).

The main purpose of the study was to investigate whether a sulfuric acid–phosphoric acid mixture can be used for the one-step removal of aluminum and cathode material metal impurities. The results shown in Fig. 1 and 2 indicate that increasing the phosphoric acid concentration and reaction time can significantly enhance the simultaneous removal of aluminum and cathode material metals from SG. At the laboratory scale, the results are significant as high metal removals of each studied metal from SG were achieved through the single-stage mixture leaching process. The long reaction time (600 min) may affect industrial feasibility. The SG was from an industrial-sized process of black mass. The industrial samples vary significantly; thus, no general conclusion can be drawn. Nonetheless, based on the leaching results, significant removals of both aluminum (90.8%) and cathode material metals (97.7–99.5%)

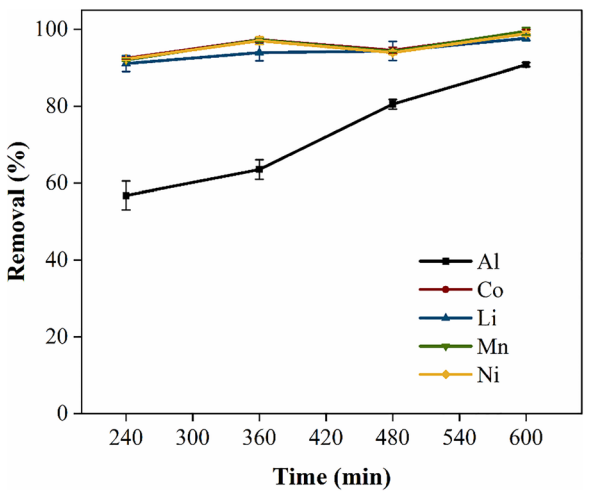

Fig. 2 Effect of reaction time (240–600 min) on simultaneous impurity removal from SG by sulfuric acid–phosphoric acid mixture (other factors: sulfuric acid: 2.75 mol L^{-1}; phosphoric acid: 0.5 mol L^{-1}; temperature: 100 °C; L/S ratio: 10 mL g^{-1}). Error bars represent experimental points of replicates (n = 2).

were achieved by the mixture leaching. In Section 3.2, samples are characterized to verify the proposed pathways.

3.2. Characterization of spent graphite purified *via* acid mixture leaching

To ensure the functionality and understand the effect of the acid mixture as a leaching agent for SG purification, samples were characterized using various techniques. First, XRD patterns were collected to identify the phases, and FESEM-EDS to study the morphologies of the samples. XPS and FTIR were used to determine the surface species and functional groups. Carbon content and residual impurities were analyzed using ICP–OES, elemental CHNS(O) analyzer, and TG.

3.2.1. Identification of the phases by XRD. Fig. 3a shows diffraction patterns of untreated SG, sulfuric acid-purified SG (2.75 mol L^{-1}, 240 min), sulfuric acid–phosphoric acid purified SG (2.75 mol L^{-1} H_2SO_4 – 0.5 mol L^{-1} H_3PO_4, 240 min), and sulfuric acid–phosphoric acid-purified SG (2.75 mol L^{-1} H_2SO_4 – 0.5 mol L^{-1} H_3PO_4, 600 min), along with ICDD references. All samples had characteristic diffraction peaks corresponding to graphite (ICDD 01-086-7889) with a hexagonal crystal structure. According to the diffractograms, the untreated SG contains lithium cobalt manganese nickel oxide (ICDD 04-026-8866) and aluminum oxide hydroxide (boehmite) (ICDD 04-010-5683) as impurities. However, the concentrations of the impurities were small (Table 1). Therefore, it was difficult to identify the correct phases for the residual impurities. Aluminum oxide hydroxide may originate from the separators used in LIBs,[45,46] or aluminum may originate from the residues of aluminum current collectors.[47] Lithium cobalt manganese nickel oxide is from the residual cathode active material.[48] The phases of other impurities could not be detected by XRD. As the concentrations were small, this does not exclude the possibility of other phases.

The XRD patterns shown in Fig. 3a show that lithium cobalt manganese nickel oxide disappeared completely from each of the treated samples, indicating total removal of cathode material metals. Aluminum oxide hydroxide peaks were visible in the sulfuric acid-treated sample, but the intensity of these peaks decreased when the sample was treated with the sulfuric acid–phosphoric acid mixture with a 240 min reaction time. The peaks disappeared completely with a 600 min reaction time, as expected based on the leaching results shown in Fig. 2. In addition, no new diffraction peaks were detected in the sample, indicating that impurities did not form any insoluble precipitates with phosphoric acid.

Enlargement of the characteristic peak of the (002) crystal plane at 25.8–27° (Fig. 3b) shows a shifting of the 2θ value toward the commercial spherical graphite (26.43°) from the untreated (26.50°) to the treated samples. The 2θ value for sulfuric acid-purified SG was 26.45°, and for sulfuric acid-phosphoric acid-purified SG (600 min), it was 26.43°. These diffraction angles (in radians) can be used to determine the interplanar spacings (d_{002}), using Bragg's Equation ($d_{002} = \lambda 2 \sin\theta_{002}$),[49,50] where λ is the wavelength of CuKα1 radiation (0.154060 nm). Electrochemical performance is affected by the

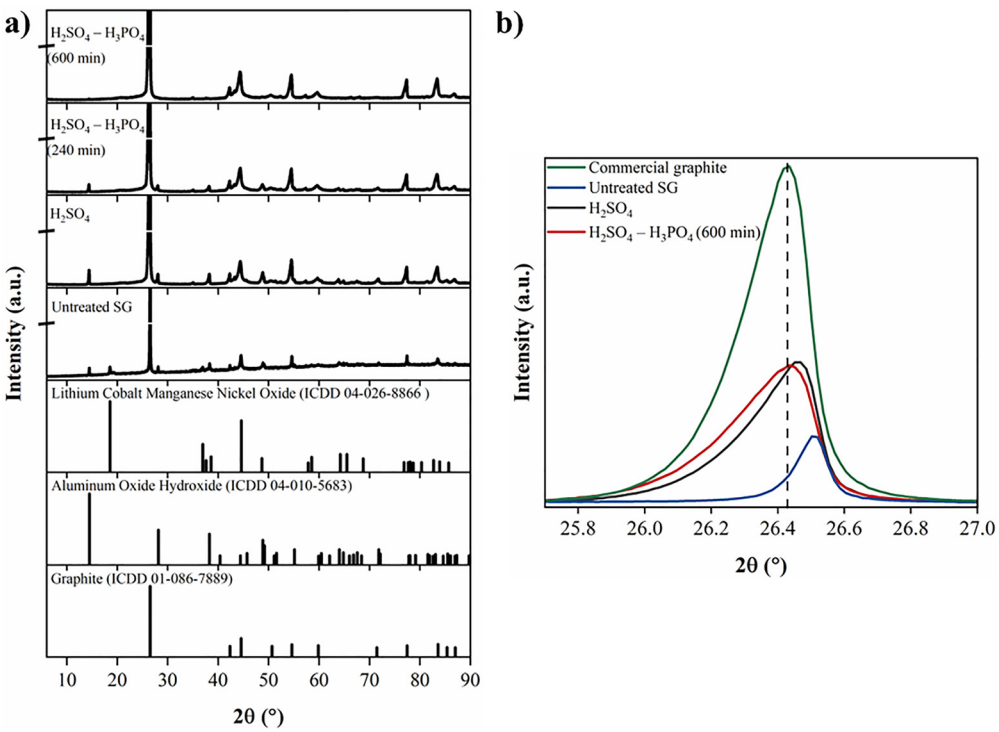

Fig. 3 (a) XRD patterns of untreated SG, sulfuric acid-purified SG (2.75 mol L^{-1}, 240 min), sulfuric acid–phosphoric acid purified SG (2.75 mol L^{-1} H_2SO_4–0.5 mol L^{-1} H_3PO_4, 240 min), and sulfuric acid–phosphoric acid purified SG (2.75 mol L^{-1} H_2SO_4–0.5 mol L^{-1} H_3PO_4, 600 min), along with ICDD references; (b) local enlargement of the characteristic diffraction peak (002) of graphite at 2θ of 25.8–27°.

interplanar spacing. Therefore, the interplanar spacing should be close to battery-grade commercial graphite if the SG is recycled back to batteries. The diffraction peaks shifted closer to commercial graphite, indicating that the interplanar spacings of treated SG samples are also closer to commercial graphite values. Fig. 3b also shows a slight increase in intensity, indicating better crystallinity compared to the untreated SG. The crystallinity may be further improved, for example, by thermal treatment.[15,25]

3.2.2. Morphology by FESEM-EDS. FESEM images with 5000× magnification were taken to characterize the morphology (Fig. 4a–d), and EDS mapping was conducted to analyze the surface impurities (Fig. 5a–c). The EDS spectra and map sum spectrums are shown in S2–S5. In the untreated sample (Fig. 4a and 5a), most surface impurities containing aluminum and oxygen were seen with plate-like particle structures. The surface of the untreated SG also contained cathode material metals (cobalt, manganese, nickel) in addition to fluorine, sulfur, and phosphorus (Fig. 5a). The fluorine may be from binder (typically polyvinylidene fluoride (PVDF)) or electrolyte salt (*e.g.*, lithium hexafluorophosphate) residues. Similarly, phosphorus may come, *e.g.*, from the electrolyte salt.[48] Plate-like aluminum impurities were seen in the sulfuric acid-purified sample (Fig. 4b; see EDS mapping, Fig. 5b). The amount decreased notably when the sample was purified with the sulfuric acid–phosphoric acid mixture (2.75 mol L^{-1} H_2SO_4–0.5 mol L^{-1} H_3PO_4, 600 min) (Fig. 4c). The EDS mapping (Fig. 5c) and map sun spectrum (Fig. S5) of this sample show only a small number of impurities containing aluminum and oxygen. The results are consistent with the leaching results (Fig. 2) and the XRD analysis (Fig. 3). In contrast, other surface impurities were not detected. The amount of surface impurities was low, as they could not be identified by XRD (Fig. 3). Based on the FESEM images, the commercial graphite reference sample was spheroidized graphite (Fig. 4d; see EDS mapping, Fig. S1). A similar morphology was seen in the spent and purified graphite samples.

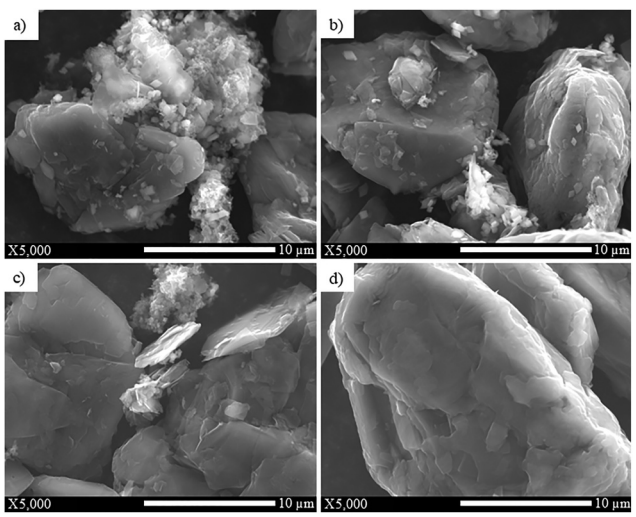

Fig. 4 FESEM image of (a) untreated SG, (b) sulfuric acid purified SG (2.75 mol L^{-1}, 240 min), (c) sulfuric acid–phosphoric acid purified SG (2.75 mol L^{-1} H_2SO_4–0.5 mol L^{-1} H_3PO_4, 600 min), and (d) commercial graphite.

3.2.3. Surface species analysis by XPS. XPS survey of untreated SG and sulfuric acid–phosphoric acid (2.75 mol L^{-1} H_2SO_4–0.5 mol L^{-1} H_3PO_4, 600 min) treated SG is shown in Fig. 6. To analyze surface species, high-resolution spectra are shown in Fig. 7a for the untreated SG and in Fig. 7b for the sulfuric acid–phosphoric acid treated sample (see high resolution spectra for other elements in Fig. S6). The intensities of each element have been presented on the same scale for comparison. Peak positions and corresponding atomic%, analyzed by the Avantage program, are shown in Table S3.

Based on Fig. 6 and 7, both samples primarily consist of C 1s peaks. C 1s was fitted into five components. The dominant surface species in both samples was the graphitic carbon at 284.8 eV.[16,17,51] Based on scientific literature,[16,17,51] it is suggested that other species are C–C or C–H (285.8–285.9 eV), C–O (286.5 eV), C═O (288.7–288.8 eV), and CF_2 at 291.1 eV. The F 1s peak showed the presence of organic fluorine (3.6 at%) at BE of 688.0 eV,[52,53] which was also detected in the purified SG (3.9 at%), indicating that the peak at 291.1 eV corresponds to the CF_2 species. Hence, the XPS supports EDS mapping shown in Fig. 5. Other primary impurity components were oxygen and aluminum. The Al 2p peaks related to aluminum oxide[52] were significantly reduced from 3.8 at% to 0.7 at% by the treatment. The XPS survey shown in Fig. 6 revealed quite small peaks (atomic% < 0.1) of cathode material metals (nickel, manganese, and cobalt) in the untreated SG sample, but almost unseen in the treated SG sample. The XPS spectra of the purified sample mainly consists of carbon, oxygen, and fluorine, which is consistent with other characterization results and supports proposed reaction pathways.

3.2.4. Functional groups analysis by FTIR. The FTIR analysis was performed for the untreated SG, sulfuric acid–phosphoric acid (2.75 mol L^{-1} H_2SO_4–0.5 mol L^{-1} H_3PO_4, 600 min) purified SG, and commercial graphite to study the possible changes in functional groups in purified SG (Fig. 8). The samples were diluted with potassium bromide (1 : 100) before analysis, and the baseline was measured with potassium bromide. All samples had a band at ~2980 cm^{-1}, which can be attributed to the symmetric stretching of CH_2.[54,55] The untreated and purified SG revealed a band at 1380 cm^{-1}, which may be from organic impurities that could not be removed by the sulfuric acid–phosphoric acid leaching. For example, symmetric bending of $-CH_3$ is located at 1390–1370 cm^{-1}.[54–56] The untreated SG sample had a band at ~1073 cm^{-1} that can be attributed to the Al–O stretching of the aluminum oxide hydroxide impurity.[57] Disappearance of this band from purified SG indicates removal of Al–O containing phases, which is aligned with the leaching and other characterization results. In addition, according to the FTIR analysis, the sulfuric acid–phosphoric acid leaching did not result in the formation of new functional groups to the SG.

3.2.5. Carbon content and residual impurities. To analyze the quantity of residual impurities more accurately, the

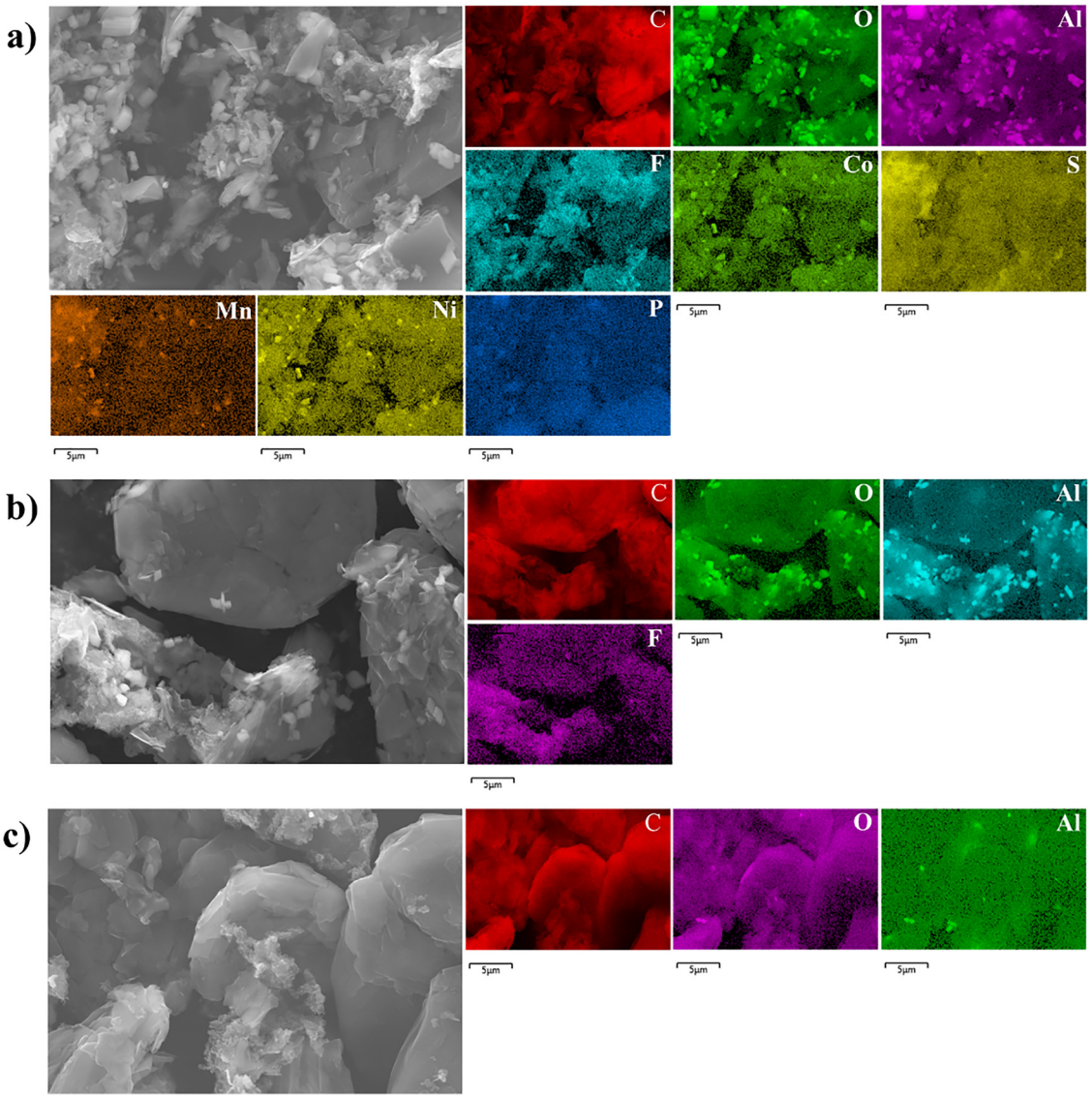

Fig. 5 FESEM-EDS mapping of (a) untreated SG, (b) sulfuric acid purified SG (2.75 mol L^{-1}, 240 min), and (c) sulfuric acid–phosphoric acid purified SG (2.75 mol L^{-1} H_2SO_4–0.5 mol L^{-1} H_3PO_4, 600 min).

samples were analyzed using ICP–OES and an elemental CHNS(O) analyzer. Based on the ICP–OES analysis in Table 1, the untreated SG contained 27.90 mg g^{-1} aluminum, 35.57 mg g^{-1} cobalt, 5.80 mg g^{-1} lithium, 33.70 mg g^{-1} manganese, 36.03 mg g^{-1}, nickel, 0.1 wt% nitrogen, 0.5 wt% hydrogen, 1.5 wt% sulfur, and 9.4 wt% oxygen. Other measured impurity concentrations were <5 mg g^{-1}. Residual impurities in purified SG samples measured by ICP–OES showed that the aluminum content decreased with 240 min sulfuric acid leaching to 27.70 mg g^{-1} (Table 3). Although sulfuric acid was not sufficient alone for aluminum removal, it was shown that the mixture of sulfuric acid–phosphoric acid increased the removal efficiency. Aluminum content was significantly decreased to 15.70 mg g^{-1} only by adding phosphoric acid (0.5 mol L^{-1}) to the system. The aluminum content was further decreased by the single-stage process with a longer reaction time (600 min), to 6.41 mg g^{-1}. The addition of phosphoric acid to the system did not affect cathode material metal removals, as they were almost completely removed in both the sulfuric acid and sulfuric acid–phosphoric acid leaching treatments.

In our previous study,[25] the aluminum content was reduced to 6.46 mg g^{-1} and the carbon content was increased from 69.2 wt% to 94.7 wt% by a two-stage acid–alkali leaching process.[25] In this study, the aluminum content of the same SG sample was reduced to 6.41 mg g^{-1}, and the carbon content was increased to almost the same level (93.0 wt%) through single-stage acid mixture leaching (Tables 3 and 4). This minimizes the needed purification steps in addition to the amount of wastewater produced. Table S4 shows the carbon content and impurity concentrations of samples with shorter reaction time (360 min and 480 min) with 0.5 mol L^{-1} phosphoric acid concentration and shorter reaction time (480 min) with

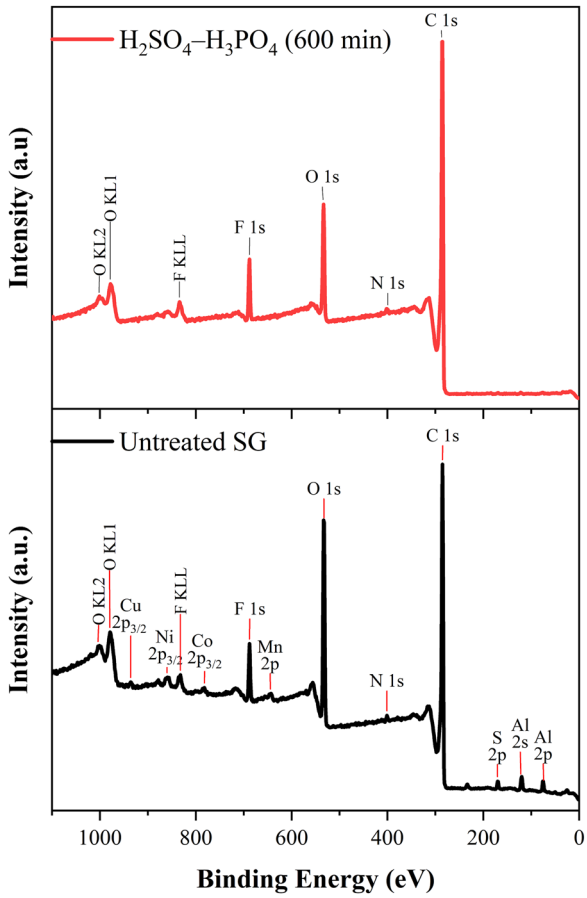

Fig. 6 XPS survey of untreated SG and sulfuric acid–phosphoric acid purified SG (2.75 mol L^{-1} H_2SO_4–0.5 mol L^{-1} H_3PO_4, 600 min).

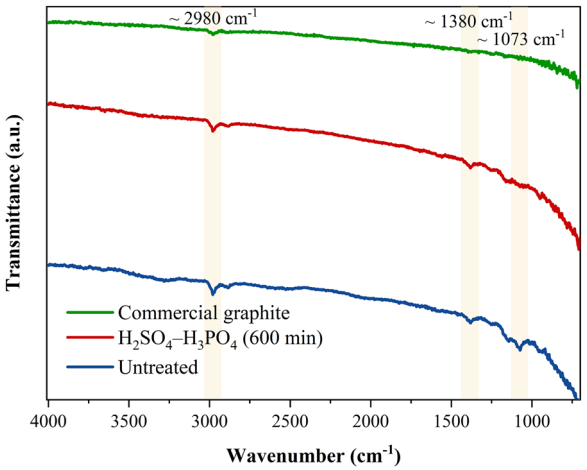

Fig. 8 FTIR spectra of untreated SG, sulfuric acid–phosphoric acid purified SG (2.75 mol L^{-1} H_2SO_4–0.5 mol L^{-1} H_3PO_4, 600 min), and commercial graphite.

0.7 mol L^{-1} phosphoric acid concentration. The carbon content of the 480 min sample (92.7 wt%) was only slightly lower compared to the 600 min sample. Table S4 also shows that higher carbon content with shorter reaction time (480 min) can be obtained, *e.g.*, by increasing the phosphoric acid concentration in the mixture to 0.7 mol L^{-1}. The residual aluminum content was 4.87 mg g^{-1} for this sample, and the carbon content was 93.6 wt%. However, this leads to an increase in the phosphate content in the acid waste.

Based on Tables 3 and 4, the remaining determined impurities in the SG sample account for 2.8% (mainly from aluminum, oxygen, and hydrogen), leaving 4.2% of impurities undetermined from the sulfuric acid–phosphoric acid (2.75 mol L^{-1} H_2SO_4–0.5 mol L^{-1} H_3PO_4, 600 min) purified SG. For example, fluorine could not be determined using ICP–OES, but EDS mapping (Fig. 5) and XPS (Fig. 6 and 7) showed its presence. As mentioned, fluorine may be from binder (typically PVDF) or electrolyte salt (*e.g.*, lithium hexafluorophosphate) residues.[48] In addition to the binder, the SG sample may also contain other organic components, such as organic solvents and plastics from separators, affecting to the purity.[58]

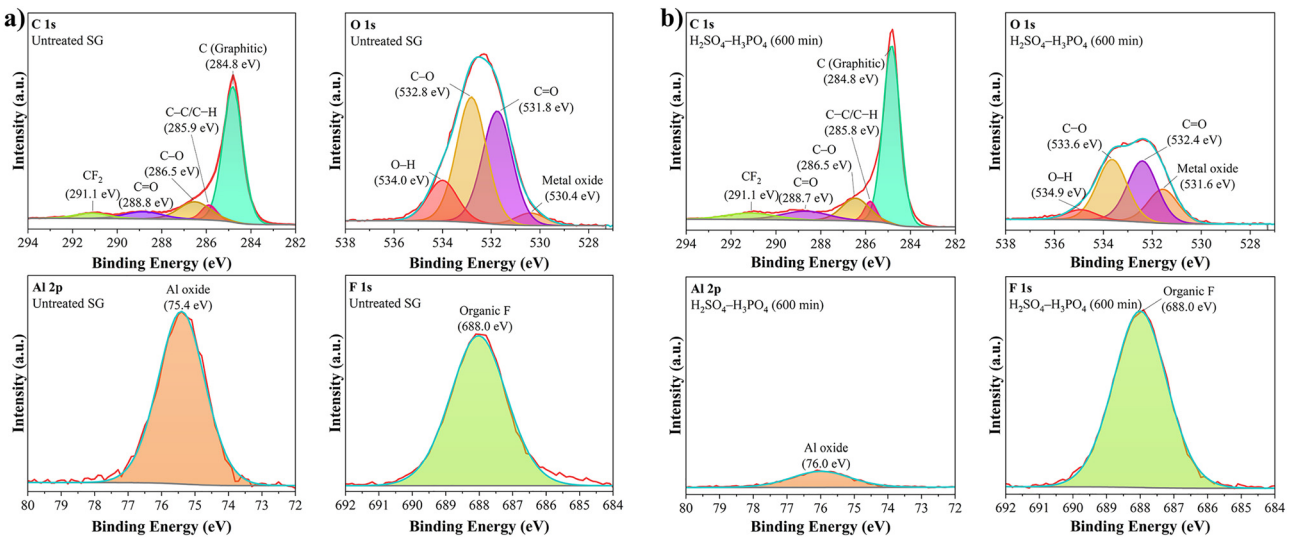

Fig. 7 High resolution spectra of (a) untreated SG, and (b) sulfuric acid–phosphoric acid purified SG (2.75 mol L^{-1} H_2SO_4–0.5 mol L^{-1} H_3PO_4, 600 min).

Table 3 Residual impurities (mg g^{-1} ± mg g^{-1}) of purified SG samples measured by ICP–OES after microwave-assisted acid digestion (n = 2)

Sample	Al (mg g^{-1})	Co (mg g^{-1})	Cu (mg g^{-1})	Li (mg g^{-1})	Mn (mg g^{-1})	Ni (mg g^{-1})	P (mg g^{-1})
H_2SO_4 (240 min)	27.70 ± 1.00	0.151 ± 0.095	0.033 ± 0.004	0.061 ± 0.030	0.142 ± 0.088	0.163 ± 0.092	0.468 ± 0.024
H_2SO_4–H_3PO_4 (240 min)	15.70 ± 2.10	0.094 ± 0.010	0.034 ± 0.000	0.033 ± 0.002	0.092 ± 0.010	0.107 ± 0.012	0.608 ± 0.010
H_2SO_4–H_3PO_4 (600 min)	6.41 ± 0.54	0.069 ± 0.008	0.024 ± 0.001	0.070 ± 0.002	0.066 ± 0.006	0.093 ± 0.003	0.657 ± 0.004

Table 4 Elemental CHNS(O) analysis (wt% ± SD) of purified SG samples (n = 6), commercial graphite (n = 3–6), and reference graphite (n = 3–9)

Sample	N (wt%)	C (wt%)	H (wt%)	S (wt%)	O (wt%)
H_2SO_4 (240 min)	0.1 ± 0.1	88.5 ± 0.5	0.4 ± 0.0	0	2.0 ± 0.0
H_2SO_4–H_3PO_4 (240 min)	0.1 ± 0.0	90.7 ± 0.6	0.3 ± 0.0	0	1.8 ± 0.1
H_2SO_4–H_3PO_4 (600 min)	0.1 ± 0.0	93.0 ± 0.4	0.3 ± 0.0	0	1.7 ± 0.1
Commercial graphite	0.1 ± 0.1	98.1 ± 0.6	0.1 ± 0.0	0	0.1 ± 0.0
Reference graphite (99.99 wt%)	0	98.7 ± 0.5	0	0	0

Furthermore, it should be noted that the uncertainty in the analytical measurements may affect the results. The carbon content of the reference graphite (99.99 wt%) was measured to be slightly lower (98.7 ± 0.5 wt%) by the elemental analyzer (Table 4).

TGA under a nitrogen atmosphere was used to determine the quantity of residual organic impurities in sulfuric acid–phosphoric acid purified SG (2.75 mol L^{-1} H_2SO_4–0.5 mol L^{-1} H_3PO_4, 600 min). An inert nitrogen atmosphere was used to prevent the graphite reacting. The weight loss of 4.5% of the sulfuric acid-phosphoric acid purified sample was observed at 200–500 °C (Fig. 9). Based on scientific literature, this mass loss can be attributed to decomposition of organic impurities.[17,58,59] For example, Golmohammadzadeh *et al.*[58] reported that the common binder PVDF decomposes at 405–485 °C, while Jaleh and Jabbari[59] reported the decomposition of PVDF in the range of 419–560 °C. Typically, organic components are removed in the pretreatment process using thermal treatment or organic solvents.[58] However, this study focused on the simultaneous removal of metallic impurities from SG material without any pretreatment processes.

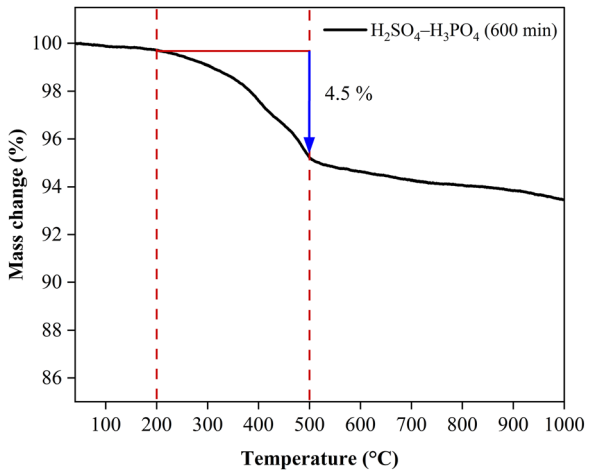

Fig. 9 TGA of sulfuric acid–phosphoric acid purified SG (2.75 mol L^{-1} H_2SO_4–0.5 mol L^{-1} H_3PO_4, 600 min) under a nitrogen atmosphere.

Comparison of the proposed purification treatment to the process presented in the Scientific literature is shown in Table 5. For comparability, only publications that reported carbon content and studied SG samples from spent batteries containing aluminum and cathode metal impurities were considered. In the literature exists a limited amount of publications fulfilling those selection criteria. Yet, it should be noted that, *e.g.*, the impurity phases may vary. In the literature, reduction of aluminum and cathode material metal contents in SG has been applied, *e.g.*, by a sulfation roasting process before leaching by Gao *et al.*[21,24] The sulfation roasting process converts cathode material metals and elemental metals into water-soluble sulfates, which are removed by sulfuric acid leaching.[21] Alternatively, Zhu *et al.*[26,60] used ammonium fluoride to convert impurities into water-soluble complexes by the fluorination roasting, which were removed from SG using a water leaching process. Li *et al.*[23] on the other hand, used sodium hydroxide roasting and hydrochloric acid leaching for the SG purification. The roasting processes have the advantages of converting impurities into soluble forms, resulting in high purities after leaching.

Compared to the other samples shown in Table 5, the carbon content of the untreated SG in this study was significantly lower (69.2 wt%). Therefore, the increase in purity was notably higher than in these other studies. In our previous study,[25] an SG sample with similar impurities (*e.g.*, aluminum oxide hydroxide) but with higher initial carbon content (89.9 wt%) was also purified using a two-stage acid–alkali leaching process. The carbon content was upgraded to 97.1 wt% by two-stage leaching. Thus, SG with higher initial purity could be upgraded to the same level of purity as reported in literature through the mixture leaching process. The advantage of the developed process is that there are fewer process steps compared to these other processes, and the temperature

Table 5 Comparison of the proposed mixture leaching method to the purification treatments proposed in the Scientific literature

Process	Chemicals	SG (wt%)	Purified SG (wt%)	Ref.
Sulfation roasting (200 °C)–acid leaching (90 °C)	H_2SO_4	96.8	99.4	24
Sulfation roasting (250 °C)–acid leaching (90 °C)	H_2SO_4	88.1	98.9	21
Fluorination roasting (200 °C)–water leaching (60 °C)	NH_4F	94.2	99.98	26
Alkali roasting (500 °C)–acid leaching	NaOH, HCl	81.9	99.9	23
Acid leaching (60 °C)	HF	94.8	99.5	61
Acid leaching (50 °C)–alkali leaching (100 °C)	H_2SO_4–H_2O_2, NaOH	69.2	94.7	25
Acid leaching (50 °C)–alkali leaching (100 °C)	H_2SO_4–H_2O_2, NaOH	89.9	97.1	25
Acid mixture leaching (100 °C)	H_2SO_4–H_3PO_4	69.2	93.0	This study

is lower (100 °C) compared to the roasting processes (200–500 °C). In addition, halogen-containing chemicals are not used. It should also be noted that, depending on the aluminum phase and experimental conditions, sulfuric acid leaching can remove aluminum impurities to some extent, as shown in Wei *et al.*[17] and Ma *et al.*[62] studies. However, this study showed that the removal can be accelerated significantly by adding phosphoric acid to the system.

Further research should be conducted to determine whether leachate can be directed toward aluminum- and iron-containing black mass leaching. Aluminum and iron impurities could be removed from the pregnant leach solution (PLS) using phosphate precipitation. Also, the presence of phosphate ions reduces the co-precipitation of lithium, nickel, cobalt, and manganese.[63] Nonetheless, all results support the finding that phosphoric acid addition to sulfuric acid solution increases the possibility of simultaneous removal of aluminum and cathode material metals from SG.

3.3. Lithium phosphate as an alternative phosphate source

The LIB industry, where demand for lithium is high, usually uses lithium hydroxide or lithium carbonate.[39] Yet, lithium carbonate precipitation often leaves notable lithium concentrations after precipitation. From low-concentration solutions, lithium is often precipitated as lithium phosphate due to its low solubility.[38,39] However, for recovered lithium phosphate, there are not many applications, and the market demand is small.[39] In this study, lithium phosphate was directly investigated as an alternative phosphate source in the mixture without any separate conversion reaction for SG purification. Lithium

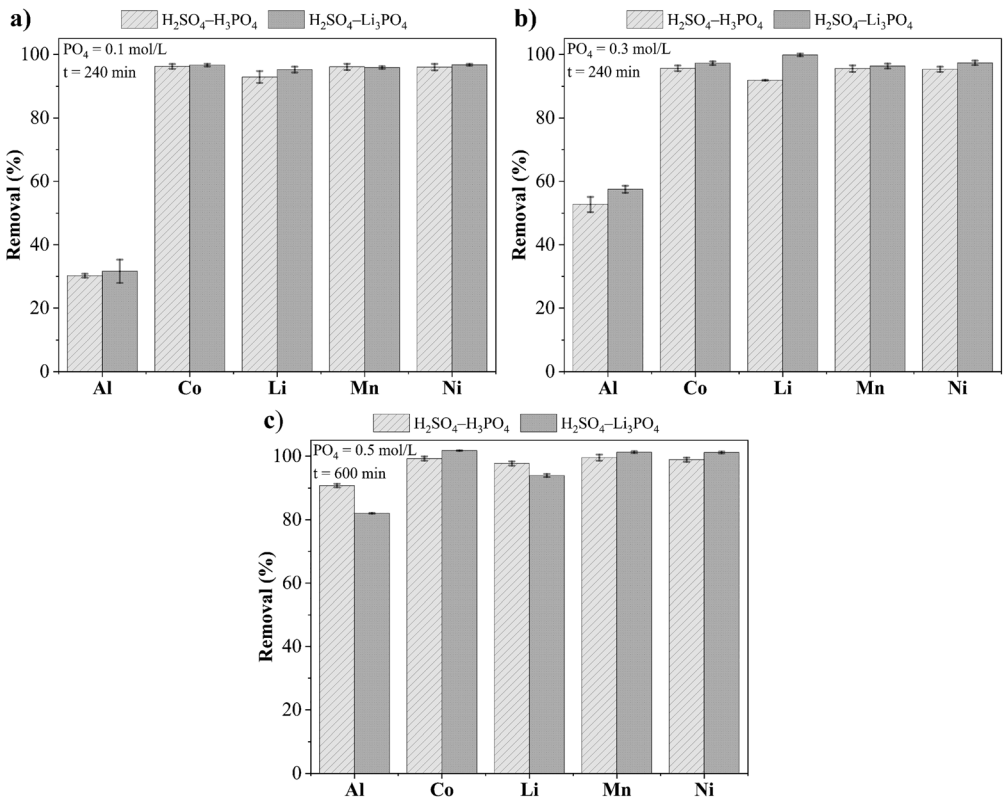

Fig. 10 Comparison of phosphoric acid and lithium phosphate as a phosphate source in the mixture with sulfuric acid, with (a) 0.1 mol L^{-1} phosphate concentration and 240 min reaction time, (b) 0.3 mol L^{-1} phosphate concentration and 240 min reaction time, and (c) 0.5 mol L^{-1} phosphate concentration and 600 min reaction time. Other factors were kept constant: sulfuric acid: 2.75 mol L^{-1}; temperature: 100 °C; and L/S ratio: 10 mL g^{-1}. Error bars represent replicates (n = 2).

Table 6 Residual impurities (mg g^{-1} ± mg g^{-1}) of purified SG samples measured by ICP–OES after microwave-assisted acid digestion (n = 2)

Mixture	PO_4 (mol L^{-1})	Time (min)	Al (mg g^{-1})	Co (mg g^{-1})	Cu (mg g^{-1})	Li (mg g^{-1})	Mn (mg g^{-1})	Ni (mg g^{-1})	P (mg g^{-1})
H_2SO_4–H_3PO_4	0.1	240	25.16 ± 0.29	0.092 ± 0.004	0.036 ± 0.001	0.076 ± 0.002	0.087 ± 0.003	0.098 ± 0.006	0.559 ± 0.004
H_2SO_4–Li_3PO_4	0.1	240	24.69 ± 1.27	0.110 ± 0.015	0.034 ± 0.004	0.082 ± 0.003	0.104 ± 0.014	0.114 ± 0.016	0.553 ± 0.007
H_2SO_4–H_3PO_4	0.3	240	17.66 ± 2.06	0.095 ± 0.016	0.035 ± 0.001	0.077 ± 0.002	0.092 ± 0.018	0.100 ± 0.015	0.604 ± 0.008
H_2SO_4–Li_3PO_4	0.3	240	18.37 ± 1.38	0.088 ± 0.004	0.038 ± 0.001	0.085 ± 0.000	0.083 ± 0.003	0.095 ± 0.004	0.592 ± 0.002
H_2SO_4–Li_3PO_4	0.5	600	8.77 ± 0.03	0.085 ± 0.002	0.037 ± 0.000	0.097 ± 0.003	0.082 ± 0.003	0.100 ± 0.002	0.633 ± 0.006

phosphate was prepared from the lithium sulfate filtrate from cathode material precursor precipitation as described in Section 2.2.

3.3.1. Comparison of lithium phosphate and phosphoric acid as alternative phosphate sources. Lithium phosphate was investigated as an alternative phosphate source with a sulfuric acid–lithium phosphate (0.1 and 0.3 mol L^{-1}) mixture with a 240 min reaction time, and sulfuric acid–lithium phosphate (0.5 mol L^{-1}) mixture with a 600 min reaction time. The results were compared to corresponding sulfuric acid–phosphoric acid results and are shown in Fig. 10a–c. Both mixtures exhibit a similar trend in terms of aluminum and cathode material removal from the SG. Increasing phosphate concentration and reaction time in the system increases the removal of aluminum, while the cathode material metals (lithium, nickel, manganese, and cobalt) were removed almost completely (>92%) in each experiment. In the sulfuric acid–lithium phosphate mixture, sulfuric acid provides strongly acidic conditions (pH < 0). Simplified, based on eqn (2) (shown in Section 3.1.1) and (4), phosphates from lithium phosphate are present as phosphoric acid in the mixture. As stated in Section 3.1.1, phosphoric acid has the capability to complex aluminum, removing aluminum impurities from SG. Simultaneously, cathode material metals are removed.

$$2Li_3PO_4(s) + 3H_2SO_4(aq) \rightarrow 3Li_2SO_4(aq) + 2H_3PO_4(aq) \quad (5)$$

3.3.2. Characterization of the residues. Tables 5 and 6 show the carbon and residual impurity content of the purified SG samples analyzed using ICP–OES and an elemental CHNS(O) analyzer. The residual impurities show a similar trend to the removals calculated from the acid leachates (Fig. 10a–c). When the concentration of the phosphate source was 0.5 mol L^{-1} and the reaction time was 600 min, the aluminum content decreased from 27.90 mg g^{-1} to 6.41 mg g^{-1} by the sulfuric acid–phosphoric acid mixture (see Table 3). Under the same reaction conditions, the aluminum content was decreased to 8.77 mg g^{-1} with a sulfuric acid–lithium phosphate mixture (see Table 6). The ICP–OES results of the solid samples also revealed that cathode material metals and copper were equally reduced almost completely in the SG samples (Tables 3 and 5). The same trend can be seen for the other samples. The carbon content analysis by the elemental CHNS(O) analyzer revealed that by the sulfuric acid–phosphoric acid mixture treatment, the carbon content of the SG increased from 69.2 to 93.0 ± 0.4 wt% (Table 3), while by the sulfuric acid–lithium phosphate mixture treatment increased the carbon content of the SG almost to the same level (92.3 ± 0.3 wt%) (Table 7).

The XRD patterns of sulfuric acid–lithium phosphate (2.75 mol L^{-1} H_2SO_4–0.5 mol L^{-1} Li_3PO_4, 600 min) purified SG are shown in Fig. 11a. The sample exhibited mainly graphite (ICDD 01-086-7889) phase and only a small amount of aluminum oxide hydroxide (ICDD 04-010-5683), and aluminum oxide (ICDD 04-015-8609) were detected. These aluminum phases could not be detected in the corresponding sulfuric acid–phosphoric acid purified sample (Fig. 3a), even though the residual aluminum contents were almost at the same level (see Table 6). In addition, new peaks were not detected in the sulfuric acid–lithium phosphate purified SG (2.75 mol L^{-1} H_2SO_4–0.5 mol L^{-1} Li_3PO_4, 600 min) sample. Lithium cobalt manganese nickel oxide (ICDD 04-026-8866), which was identified in the untreated sample (Fig. 3a), could not be detected in the sulfuric acid- lithium phosphate treated SG, indicating the removal of cathode material metals. These results are consistent with the ICP–OES results shown in Table 6. The EDS mapping results (Fig. 11a and b) revealed only tiny amounts of aluminum impurities, in addition to organic impurities (see EDS spectra and map sum spectrum in Fig. S7 and S8).

All results indicate that the sulfuric acid–lithium phosphate mixture has a similar capability to simultaneously remove aluminum and cathode material metal impurities from SG as the sulfuric acid–phosphoric mixture. This study offers a new possible application for lithium phosphate without requiring a separate conversion reaction. As mentioned in Section 3.2.5, this phosphate-containing acid leachate after SG purification could potentially be implemented for aluminum- and iron-rich

Table 7 Elemental CHNS(O) analysis (wt% ± SD) of purified SG samples and commercial graphite (n = 6)

Mixture	PO_4 (mol L^{-1})	Time (min)	N (wt%)	C (wt%)	H (wt%)	S (wt%)	O (wt%)
H_2SO_4–H_3PO_4	0.1	240	0	88.8 ± 0.4	0.5 ± 0.2	0	2.2 ± 0.1
H_2SO_4–Li_3PO_4	0.1	240	0.1 ± 0.1	88.5 ± 0.9	0.4 ± 0.1	0	2.1 ± 0.0
H_2SO_4–H_3PO_4	0.3	240	0	90.5 ± 0.4	0.4 ± 0.1	0	2.0 ± 0.0
H_2SO_4–Li_3PO_4	0.3	240	0.1 ± 0.1	90.7 ± 0.8	0.4 ± 0.0	0	2.0 ± 0.1
H_2SO_4–Li_3PO_4	0.5	600	0	92.3 ± 0.3	0.3 ± 0.0	0	2.2 ± 0.1

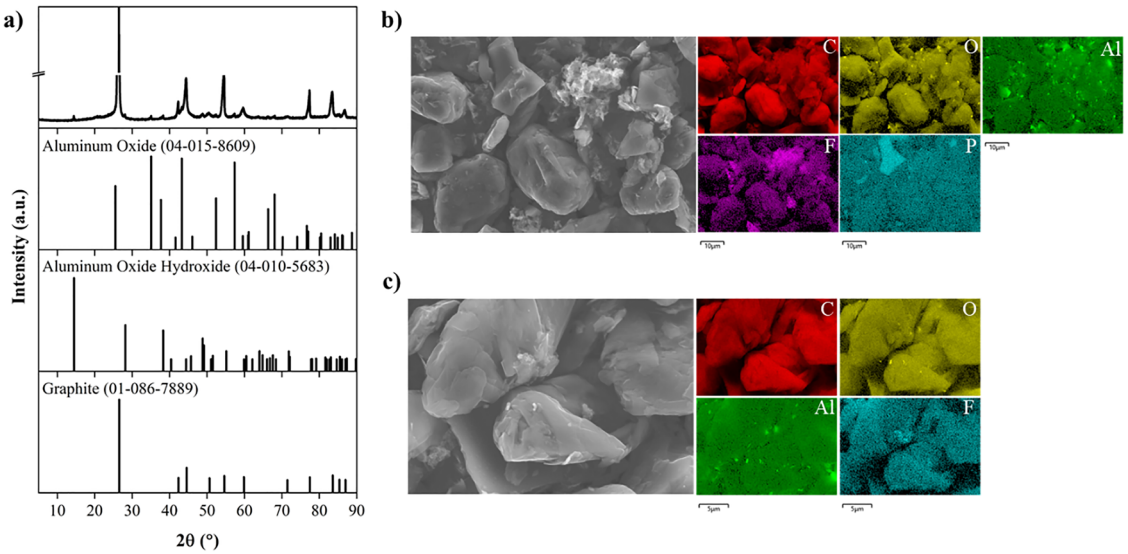

Fig. 11 (a) XRD patterns, and (b) and (c) EDS mapping of sulfuric acid–lithium phosphate purified SG (2.75 mol L^{-1} H_2SO_4–0.5 mol L^{-1} Li_3PO_4, 600 min).

black mass leaching. The presence of phosphate ions could enhance the removal of aluminum and iron impurities from the lithium-nickel-manganese-cobalt (NMC) containing PLS.[63] After separating these impurities, the NMC metals can be recovered from the PLS into separate sulfate solutions using, for example, ion exchange.[64]

4. Conclusion

In this study, the effects of leaching conditions on cathode material metals and aluminum removal from the SG were studied using a mixture of sulfuric acid and phosphate sources *via* a one-step purification process. Without a phosphate source, aluminum was removed by only 17.8% from SG. Increasing the phosphoric acid concentration (0–0.7 mol L^{-1}) increased the aluminum removal rate up to 67.2%. To avoid recyclability issues of the acid waste, a 0.5 mol L^{-1} phosphoric acid concentration was selected for further studies. With a longer reaction time (600 min, 2.75 mol L^{-1} H_2SO_4–0.5 mol L^{-1} H_3PO_4), the aluminum removal from SG was further increased to 90.8%. In this experiment, the removal of lithium, nickel, cobalt, and manganese was between 97.7% and 99.5%. Furthermore, in this single stage leaching procedure, the carbon content increased from 69.2 wt% to 93.0 wt%.

Analysis and characterization of the purified SG samples confirmed that using sulfuric acid–phosphoric acid leaching can simultaneously remove aluminum and cathode material metals from SG. Thermal treatment after mixture leaching treatment could be the next step to remove organic impurities and reconstruct the graphite to obtain battery-grade graphite. Additionally, lithium phosphate was studied as an alternative phosphate source to replace phosphoric acid in the mixture. Sulfuric acid (2.75 mol L^{-1})–lithium phosphate (0.5 mol L^{-1}) mixture with a reaction time of 600 min significantly increased the carbon content up to 92.3 wt%. The results demonstrated comparable SG purification capabilities. This provides a new application opportunity for lithium phosphate without converting it into more widely used raw materials, such as lithium hydroxide. Further research can be conducted to direct acid waste for the black mass leaching stage.

Author contributions

Venla Rantala: conceptualization, formal analysis, investigation, methodology, visualization, writing – original draft, writing – review & editing. Toni Kauppinen: conceptualization, formal analysis, investigation, methodology, visualization, writing – original draft, writing – review & editing. Tao Hu: investigation, writing – review & editing. Ali Huerta Flores: investigation, writing – review & editing. Anne Heponiemi: investigation, writing – review & editing. Ulla Lassi: conceptualization, funding acquisition, project administration, supervision, writing – review & editing. Sari Tuomikoski: conceptualization, project administration, supervision, writing – review & editing.

Conflicts of interest

There are no conflicts to declare.

Data availability

Data for this article is available in CSC's Fairdata IDA repository at https://doi.org/10.23729/fd-b9d659ba-72ba-3a78-ad9e-b1e8c602d586.

Supplementary information (SI) includes removals (%) shown in Fig. 1 and 2, FESEM-EDS results (elemental mappings, EDS spectra, and map sum spectrum), XPS results, ICP-OES results, and elemental analysis (CHNS(O)) results. See DOI: https://doi.org/10.1039/d5ma01222h.

Acknowledgements

This work was supported by Business Finland granted BATCircle3.0 (2196/31/2024), and EU/Interreg Aurora granted EcoLIB (20357954) projects. The authors thank BSc Antti Kananen for conducting the preliminary experiments. The authors also thank MSc Hansika Rathnayake Mudiyanselage and Mikko Häkkinen for the microwave-assisted acid digestion of the purified graphite samples. In addition, the authors thank MSc Tommi Kokkonen for conducting TG for two samples.

References

1 European Parliamentary Research Service, New EU regulatory framework for batteries: Setting sustainability requirements, 2022. Available from: https://www.europarl.europa.eu/thinktank/en/document/EPRS_BRI(2021)689337.
2 C. Dong, C. Liu, Z. Qin, J. Deng and Y. Zhu, A comprehensive overview of decommissioned lithium-ion battery recycling: Towards green and economical, *Sep. Purif. Technol.*, 2025, **354**, 128929.
3 G. Wei, Y. Liu, B. Jiao, N. Chang, M. Wu and G. Liu, *et al.*, Direct recycling of spent Li-ion batteries: Challenges and opportunities toward practical applications, *iScience*, 2023, **26**(9), 107676.
4 Y. Zhao, Y. Fu, Y. Meng, Z. Wang, J. Liu and X. Gong, Challenges and strategies of lithium-ion mass transfer in natural graphite anode, *Chem. Eng. J.*, 2024, **480**, 148047Available from: https://www.sciencedirect.com/science/article/pii/S1385894723067797.
5 Council of the European Union, Infographic - An EU critical raw materials act for the future of EU supply chains, 2024. Available from: https://www.consilium.europa.eu/en/infographics/critical-raw-materials/.
6 Q. Cheng, B. Marchetti, X. Chen, S. Xu and X. D. Zhou, Separation, purification, regeneration and utilization of graphite recovered from spent lithium-ion batteries – A review, *J. Environ. Chem. Eng.*, 2022, **10**(2), 107312.
7 European Parliament and of the Council, REGULATION (EU) 2023/1542 OF THE EUROPEAN PARLIAMENT AND OF THE COUNCIL of 12 July 2023 concerning batteries and waste batteries, amending Directive 2008/98/EC and Regulation (EU) 2019/1020 and repealing Directive 2006/66/EC, 2023. Available from: https://data.europa.eu/eli/reg/2023/1542/oj.
8 G. Liu, L. Ma, X. Xi and Z. Nie, Efficient purification and high-quality regeneration of graphite from spent lithium-ion batteries by surfactant-assisted methanesulfonic acid, *Waste Manage.*, 2024, **178**, 105–114.
9 Y. Lai, X. Zhu, J. Li, Q. Gou, M. Li and A. Xia, *et al.*, Recovery and regeneration of anode graphite from spent lithium-ion batteries through deep eutectic solvent treatment: Structural characteristics, electrochemical performance and regeneration mechanism, *Chem. Eng. J.*, 2023, **457**, 141196.
10 X. Y. Jian, S. X. Hui, Q. Chang, H. X. Long, Y. Sun and F. X. Yong, *et al.*, The regeneration of graphite anode from spent lithium-ion batteries by washing with a nitric acid/ethanol solution, *New Carbon Mater.*, 2022, **37**(5), 1011–1020.
11 J. Li, Y. He, Y. Fu, W. Xie, Y. Feng and K. Alejandro, Hydrometallurgical enhanced liberation and recovery of anode material from spent lithium-ion batteries, *Waste Manage.*, 2021, **126**, 517–526.
12 S. H. Zheng, X. T. Wang, Z. Y. Gu, H. Y. Lü, S. Li and X. Y. Zhang, *et al.*, Direct and rapid thermal shock for recycling spent graphite in lithium-ion batteries, *J. Colloid Interface Sci.*, 2024, **667**, 111–118.
13 G. Q. Yu, M. Z. Xie, Z. H. Zheng, Z. G. Wu, H. L. Zhao and F. Q. Liu, Efficiently regenerating spent lithium battery graphite anode materials through heat treatment processes for impurity dissipation and crystal structure repair, *Resour., Conserv. Recycl.*, 2023, **199**, 107267.
14 C. Yi, Y. Yang, T. Zhang, X. Wu, W. Sun and L. Yi, A green and facile approach for regeneration of graphite from spent lithium ion battery, *J. Cleaner Prod.*, 2020, **277**, 123585.
15 Y. Gao, J. Zhang, H. Jin, G. Liang, L. Ma and Y. Chen, *et al.*, Regenerating spent graphite from scrapped lithium-ion battery by high-temperature treatment, *Carbon*, 2022, **189**, 493–502Available from: https://linkinghub.elsevier.com/retrieve/pii/S0008622321012124.
16 Q. Chen, L. Huang, J. Liu, Y. Luo and Y. Chen, A new approach to regenerate high-performance graphite from spent lithium-ion batteries, *Carbon*, 2022, **189**, 293–304.
17 X. Wei, Z. Guo, Y. Zhao, Y. Sun, A. Hankin and M. Titirici, Recovery of graphite from industrial lithium-ion battery black mass, *RSC Sustainability*, 2025, **3**(1), 264–274.
18 A. Chernyaev, A. Kobets, K. Liivand, F. Tesfaye, P. M. Hannula and T. Kallio, *et al.*, Graphite recovery from waste Li-ion battery black mass for direct re-use, *Miner. Eng.*, 2024, **208**, 108587.
19 M. Abdollahifar, S. Doose, H. Cavers and A. Kwade, Graphite Recycling from End-of-Life Lithium-Ion Batteries: Processes and Applications, *Adv. Mater. Technol.*, 2023, **8**(2), 2200368, DOI: 10.1002/admt.202200368.
20 C. Chang, K. Sun, Y. Liu, H. Wang and F. Li, Regeneration of graphite and manganese carbonate from spent lithium-ion batteries for electric vehicles, *Ionics*, 2022, **28**, 2239–2246, DOI: 10.1007/s11581-022-04501-x.
21 Y. Gao, J. Zhang, Y. Chen, L. Wang and C. Wang, Graphite regenerating from retired (LFP) lithium-ion battery: Phase transformation mechanism of impurities in low-temperature sulfation roasting process, *Renewable Energy*, 2023, **204**, 290–299.
22 X. Xie, W. Fan, J. Zhang, R. Ma, Y. Chen and C. Wang, Regeneration of graphite anode from spent lithium iron phosphate batteries: Microstructure and morphology evolution at different thermal-repair temperature, *Powder Technol.*, 2023, **430**, 118998.
23 Y. Li, W. Lv, H. Zhao, Y. Xie, D. Ruan and Z. Sun, Regeneration of anode materials from complex graphite residue in spent lithium-ion battery recycling process, *Green Chem.*, 2022, **24**(23), 9315–9328.

24 Y. Gao, C. Wang, J. Zhang, Q. Jing, B. Ma and Y. Chen, *et al.*, Graphite Recycling from the Spent Lithium-Ion Batteries by Sulfuric Acid Curing-Leaching Combined with High-Temperature Calcination, *ACS Sustainable Chem. Eng.*, 2020, **8**(25), 9447–9455.
25 V. Rantala, T. Kauppinen, J. Välikangas, T. Hu, A. Lähde and S. Tuomikoski, *et al.*, Comparison of thermal and chemical purification methods for graphite from spent lithium-ion batteries, *Sep. Purif. Technol.*, 2025, **376**, 133992.
26 X. Zhu, J. Xiao, Q. Mao, Z. Zhang, Z. You and L. Tang, *et al.*, A promising regeneration of waste carbon residue from spent Lithium-ion batteries via low-temperature fluorination roasting and water leaching, *Chem. Eng. J.*, 2022, **430**, 132703.
27 W. Xie, Z. Wang, J. Kuang, H. Xu, S. Yi and Y. Deng, *et al.*, Fixed carbon content and reaction mechanism of natural microcrystalline graphite purified by hydrochloric acid and sodium fluoride, *Int. J. Miner. Process.*, 2016, **155**, 45–54.
28 Z. Zhang, X. Zhu, H. Hou, L. Tang, J. Xiao and Q. Zhong, Regeneration and utilization of graphite from the spent lithium-ion batteries by modified low-temperature sulfuric acid roasting, *Waste Manage.*, 2022, **150**, 30–38.
29 Y. Zhang, J. Zhang, L. Wu, L. Tan, F. Xie and J. Cheng, Extraction of lithium and aluminium from bauxite mine tailings by mixed acid treatment without roasting, *J. Hazard. Mater.*, 2021, **404**, 124044.
30 S. Shukla, A. Chernyaev and M. Lundström, Leaching kinetics of waste pharmaceutical blister package aluminium in phosphoric acid media, *Sep. Purif. Technol.*, 2024, **348**, 127760.
31 X. Chen, H. Ma, C. Luo and T. Zhou, Recovery of valuable metals from waste cathode materials of spent lithium-ion batteries using mild phosphoric acid, *J. Hazard. Mater.*, 2017, **326**, 77–86.
32 X. Zhou, W. Yang, X. Liu, J. Tang, F. Su and Z. Li, *et al.*, One-step selective separation and efficient recovery of valuable metals from mixed spent lithium batteries in the phosphoric acid system, *Waste Manage.*, 2023, **155**, 53–64.
33 L. Yang, Y. Feng, C. Wang, D. Fang, G. Yi and Z. Gao, *et al.*, Closed-loop regeneration of battery-grade $FePO_4$ from lithium extraction slag of spent Li-ion batteries via phosphoric acid mixture selective leaching, *Chem. Eng. J.*, 2022, **431**, 133232.
34 E. G. Pinna, M. C. Ruiz, M. W. Ojeda and M. H. Rodriguez, Cathodes of spent Li-ion batteries: Dissolution with phosphoric acid and recovery of lithium and cobalt from leach liquors, *Hydrometallurgy*, 2017, **167**, 66–71.
35 L. F. Guimarães, A. B. Botelho Junior and D. C. R. Espinosa, Sulfuric acid leaching of metals from waste Li-ion batteries without using reducing agent, *Miner. Eng.*, 2022, **183**, 107597.
36 R. Sattar, S. Ilyas, H. N. Bhatti and A. Ghaffar, Resource recovery of critically-rare metals by hydrometallurgical recycling of spent lithium ion batteries, *Sep. Purif. Technol.*, 2019, **209**, 725–733.
37 W. S. Chen and H. J. Ho, Recovery of Valuable Metals from Lithium-Ion Batteries NMC Cathode Waste Materials by Hydrometallurgical Methods, *Metals*, 2018, **8**(5), 321.
38 D. Liu, Z. Li, L. He and Z. Zhao, Facet engineered Li_3PO_4 for lithium recovery from brines, *Desalination*, 2021, **514**, 115186.
39 Y. Song, L. He, Z. Zhao and X. Liu, Separation and recovery of lithium from Li3PO4 leaching liquor using solvent extraction with saponified D2EHPA, *Sep. Purif. Technol.*, 2019, **229**, 115823.
40 J. Shin, J. M. Jeong, J. B. Lee, N. S. Heo, H. Kwon and Y. H. Kim, *et al.*, Recovery of lithium from $LiAlO_2$ in waste box sagger through sulfation to produce Li_2SO_4 and sequential wet conversion to Li_3PO_4, LiCl and Li_2CO_3, *Hydrometallurgy*, 2023, **215**, 105988.
41 V. Rantala, M. Kokko, R. Suvela, M. Manninen, T. Hu and U. Lassi, *et al.*, Elemental Concentrations of Natural Graphite and Steelmaking Slag: Development of Microwave-Assisted Acid Digestion, *Anal. Lett.*, 2024, **57**(14), 2230–2245.
42 T. Havlík, *Hydrometallurgy: principles and applications*, Woodhead Publishing, Cambridge, (Woodhead Publishing in materials), 2008.
43 R. F. Mortlock, A. T. Bell and C. J. Radke, Phosphorus-31 and aluminum-27 NMR investigations of highly acidic, aqueous solutions containing aluminum and phosphorus, *J. Phys. Chem.*, 1993, **97**(3), 767–774.
44 J. Rumble, T. J. Bruno and M. J. Doa, *CRC Handbook of Chemistry and Physics*, Chapman & Hall/CRC Press, Boca Raton, FL, 102nd edn, 2021.
45 J. Holtmann, M. Schäfer, A. Niemöller, M. Winter, A. Lex-Balducci and S. Obeidi, Boehmite-based ceramic separator for lithium-ion batteries, *J. Appl. Electrochem.*, 2016, **46**(1), 69–76, DOI: 10.1007/s10800-015-0895-z.
46 Y. Wang, Q. Wang, Y. Lan, Z. Song, J. Luo and X. Wei, *et al.*, Aqueous aluminide ceramic coating polyethylene separators for lithium-ion batteries, *Solid State Ionics*, 2020, **345**, 115188Available from: https://www.sciencedirect.com/science/article/pii/S0167273819309749.
47 K. K. Jena, A. AlFantazi and A. T. Mayyas, Comprehensive Review on Concept and Recycling Evolution of Lithium-Ion Batteries (LIBs), *Energy Fuels*, 2021, **35**(22), 18257–18284, DOI: 10.1021/acs.energyfuels.1c02489.
48 G. S. Jun, L. W. Feng, F. D. Ju and L. X. Guang, Research progress on recovering the components of spent Li-ion batteries, *New Carbon Mater.*, 2022, **37**(3), 435–460.
49 R. L. Snyder, X-Ray Diffraction, 1999.
50 C. N. Barnakov, G. P. Khokhlova, V. Y. Malysheva, A. N. Popova and Z. R. Ismagilov, X-ray diffraction analysis of the crystal structures of different graphites, *Solid Fuel Chem.*, 2015, **49**(1), 25–29.
51 D. J. Morgan, Comments on the XPS Analysis of Carbon Materials, *C*, 2021, **7**(3), 51.
52 C. Liu, J. Long, Y. Gao, H. Liu, W. Luo and X. Wang, Microwave low-temperature treatment – Step leaching process for recovering black mass from spent lithium-ion batteries, *J. Environ. Chem. Eng.*, 2023, **11**(3), 109759.
53 R. Dedryvère, H. Martinez, S. Leroy, D. Lemordant, F. Bonhomme and P. Biensan, *et al.*, Surface film formation on electrodes in a $LiCoO_2$/graphite cell: A step by step XPS study, *J. Power Sources*, 2007, **174**(2), 462–468.

54 P. J. Larkin, IR and Raman Spectra–Structure Correlations, in *Infrared and Raman Spectroscopy*, Elsevier, 2018, pp. 85–134.
55 M. Hesse, H. Meier and B. Zeeh, *Spectroscopic methods in organic chemistry*, Thieme, Stuttgart, (Thieme foundations in organic chemistry series), 1997.
56 J. B. Lambert, H. F. Shurvell, D. A. Lightner and R. G. Cooks, *Organic structural spectroscopy*, Prentice-Hall, Upper Saddle River (N.J.), 1998.
57 M. Del Nero, C. Galindo, R. Barillon, E. Halter and B. Madé, Surface reactivity of α-Al2O3 and mechanisms of phosphate sorption: In situ ATR-FTIR spectroscopy and ζ potential studies, *J. Colloid Interface Sci.*, 2010, **342**(2), 437–444.
58 R. Golmohammadzadeh, Z. Dimachki, W. Bryant, J. Zhang, P. Biniaz and M. Banaszak Holl, *et al.*, Removal of polyvinylidene fluoride binder and other organics for enhancing the leaching efficiency of lithium and cobalt from black mass, *J. Environ. Manage.*, 2023, **343**, 118205.
59 B. Jaleh and A. Jabbari, Evaluation of reduced graphene oxide/ZnO effect on properties of PVDF nanocomposite films, *Appl. Surf. Sci.*, 2014, **320**, 339–347.
60 X. Zhu, Q. Mao, Q. Zhong, Z. Zhang, G. Wang and L. Tang, *et al.*, A Novel Low-Temperature Fluorination Roasting Mechanism Investigation of Regenerated Spent Anode Graphite via TG-IR Analysis and Kinetic Modeling, *ACS Omega*, 2022, **7**(13), 11101–11113, DOI: 10.1021/acsomega.1c07190.
61 Z. X. Dong, J. Xiao, M. Q. Yun, Z. Z. Hua, L. Tang and Z. Q. Fan, Recycling of waste carbon residue from spent lithium-ion batteries via constant-pressure acid leaching, *Trans. Nonferrous Met. Soc. China*, 2022, **32**(5), 1691–1704.
62 X. Ma, M. Chen, B. Chen, Z. Meng and Y. Wang, High-Performance Graphite Recovered from Spent Lithium-Ion Batteries, *ACS Sustainable Chem. Eng.*, 2019, **7**(24), 19732–19738.
63 A. Chernyaev, J. Zhang, S. Seisko, M. Louhi-Kultanen and M. Lundström, Fe^{3+} and Al^{3+} removal by phosphate and hydroxide precipitation from synthetic NMC Li-ion battery leach solution, *Sci. Rep.*, 2023, **13**(1), 21445.
64 P. Kivelä, P. Ekman, E. Lappalainen, K. Haapala, P. Kauppinen and K. Ekman, Method for processing black mass to battery chemicals, EP4245869A1, 2023. Available from: https://patentimages.storage.googleapis.com/2a/fb/0f/6843ed517176fb/EP4245869A1.pdf.